Study of the Optical Characteristics of V_2O_5-Li_2O-P_2O_5 Glass System

I. I. Hussien, M. Mohsen, H. M. Hosny and M. S. Abd El Keriem

Department of Physics, Faculty of Science, Ain Shams University, 11566 Abbassia, Cairo, Egypt
Islam.Hussien@sci.asu.edu.eg

In the last two decades, several applications became more dependent on the nonlinearity phenomena in glasses, for example: laser glass has low nonlinear refractive index (n_2), while as higher values serve in optical switching. In this study, Vanadium-Lithium-Phosphate glass samples [V_2O_5-Li_2O-P_2O_5] were prepared by the melt-quenching technique. The amorphous structure of these glasses is examined by XRD analysis. The recorded reflectance and transmittance were investigated over the range from 200 to 2500 nm for the five samples. The two parts of the calculated refractive indices are estimated via an analytical technique. The dispersion parameters, such as Sellmeier gap energy based on Wemple and DiDomenico model, dispersion energy, as well as Abbe's number were deduced. From the obtained results, the parameters for absorption dispersion, namely, the optical energy gap for indirect transition as well as the Urbach energy, were extracted. Moreover, the other parameters such as: the molar refractivity, the reflection loss and density are calculated. The measured optical parameters were found to vary nonlinearly with increasing vanadium oxide (V_2O_5), in the presence of Li_2O in the phosphate matrix. In the aim of enhancing the performance in this glass system, the effects of ascending doping with a transition metal oxide (V_2O_5) on both the predicted nonlinear and the linear optical parameters, are investigated and analyzed.

1. Introduction

Historically, in 1932 Zachariasen proposed the following four rules that allowed the selection of the most suitable oxides that have tendency to form glasses;

An oxygen (O) atom is ordinarily linked to two glass forming atoms.

The oxygen polyhedra have tendency to share corners with each other (not edges or faces).

The coordination number of the glass-forming atoms is considerably small.

The polyhedra are linked in a 3D network.

In comparison with silicate and borate glasses, the peculiar and exquisite physical properties of phosphate glasses aim to promote applications in various domains.

These properties include: high thermal expansion coefficient, low melting temperature, near normal preparation temperature (glass sealing candidates), low transition temperature, significant refractive indices (n) as well as conventional high transmission in UV range (e.g. laser sensing tech., optical data transmission, etc.). The accompanying outstanding optical properties offer advantages, specifically in the molding of the optical elements and nuclear waste storage glass [1], among other technical and biological applications [2]. Though transition metal oxides have a mixed dual role, as modifiers and formers, their semiconducting properties, photo-conducting, optical absorption and electrical memory switching seem to motivate the vanadate glasses to contribute in unceasing glass systems for advanced applications. On the other hand, the hygroscopic nature of theses glasses leads to poor chemical stability; which calls for adding the alkali, transition metal or rare earth ions [3,4]. Industrial applications, based on such improvements, include: pigment manufacturing, impounding agents for hard water treatment and separation for clay processing [3,5].

From the previous work [6,7], the structural units of phosphate glasses fall into Q^n groups; where n: is the number of bridging oxygen (BO) per unit cell, Fig. (1).

These groups start with ultraphosphate (Q^3), metaphosphate (Q^2), pyrophosphate (Q^1) then orthophosphate (Q^0), creating non bridging oxygens (NBOs), upon adding modifying oxide to P_2O_5 [3,8,9,10]. According to spectroscopic analysis [11,12] transition metal ions (TMIs) in alkali phosphate glasses seem to prefer the low valence state (octahedral) than the high valance state (tetrahedral). This indicates that P-tetrahedra are the basic building blocks of vitreous phosphates which are linked through covalent BOs to the amorphous phosphate. Hence, a network of (Q^3) tetrahedral units, with three BOs bridging ($P-O-P$) and one NBO ($P=O$) for the short range structure of P_2O_5 glass. Principally, in a single component glass system, an oxygen of a very short ($P=O$) bond can be distinguished on each network configured (O^-) cation; with a purport $\pi-$ bond character, which accounts for the additional valance electrons [13]. The polymeric structure can be altered for 3D random network to a linear phosphate chain upon adding a modifier oxide (alkali or alkali earth) [3,14]. Experimental and theoretical studies [15,16] deduced that upon increasing the modifier concentration, the long chains of phosphate are reduced causing a break in the network coherency results in NBOs. The P_2O_5 glasses therefore tend to disintegrate forming structural elements, consisting of rings and chains, which reduces the oxide modified glasses to become relatively stable. The addition of vanadium pentoxide to the mixed divalent oxide phosphate glasses tends to

improve the durability of phosphate with the benefit that it can exhibit the luster and appearance of lead glass; which is costly and fragile.

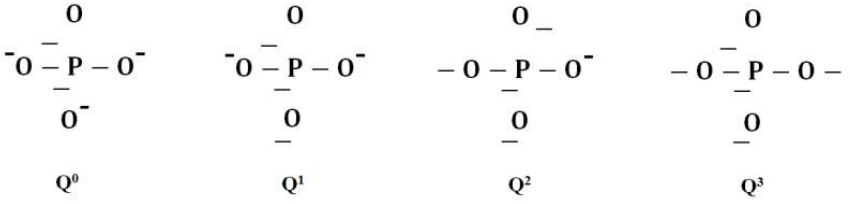

Fig. (1): Phosphate based glass tetrahedral in Q^i terminology.

2. Experimental Procedure

2.1. Preparation Method

Glassy samples of [V_2O_5 - Li_2O- P_2O_5], were prepared by the traditional melt quenching technique. These samples were prepared by mixing together appropriate amounts of $NH_4H_2PO_4$ (Aldrich. 99.997%), Li_2CO_3 (Aldrich. 99.99%) and V_2O_5 (Aldrich. 99.99%). In several earlier studies, $NH_4H_2PO_4$ and Li_2CO_3 were used to obtain P_2O_5 and Li_2O [17,18,19,20]. The above mixtures were heated at first in an electric furnace at 250°C for 1.5h, in alumina crucibles, to remove the volatile products. This was followed by further increase in temperature, up to 950°C for 1 h; with frequent stirring of the melt to ensure homogeneity. In an attempt to avoid severe shattering of the quenched samples as a direct of thermal stress, the mixtures were poured in turn on preheated 300°C stainless steel plates. Rectangular samples of thickness 3-mm were annealed for 2 h at 300°C to relieve residual internal stress and slowly cooled to room temperature.

Table (1). Percentage composition of the prepared samples

Glass Sample	Composition %		
	P_2O_5	Li_2O	V_2O_5
S_0	70	30	0
S_1	70	29.8	0.2
S_2	70	29.6	0.4
S_3	70	29	1
S_4	70	28	2

2.2. Spectrophotometric Measurements

Computer aided two-beam spectrophotometer (JASCO Corp., V – 570, Rev. 1.00 UV/VIS/NIR, Japan) was used to measure the Reflectance (R) and transmission (T) from the plane-parallel glass samples. The resolution limit of the spectrometer is $\delta\lambda$ = 2 nm. The accuracy of measuring reflectance and transmittance is $\pm$ 0.002 with the incident beam making an angle of 5.0°± 0.1° to the normal of the external sample faces. The angle of the

propagating beam through the sample is within below 5^0. The measurements were carried out at room temperature for the entire spectral range 0.19-2.5 μm (data ~ 1160 points).

3. Factors that affect the linear refractive index

There are several factors are more important influencing in the linear refractive index of oxide glasses;

1- The most important is the dependency of linear refractive index on the density (ρ) [21,22] according to the relation $[n = (C_1\rho + 1)^{1/2}]$, where ($C_1$) is a constant.

In previous studies [21] other aspects proved to be effective, among them:

a. polarizability of the first neighbor ions coordinated with it (anion),
b. field intensity $z=a^2$ (i.e., polarization power), where (z) is the ionic charge and (a) is the ionic radius,
c. coordination number of the ion,
f. fundamental NBO's,
g. the oxide ion's electronic polarizability,
h. optical basicity of the material.

Moreover, the dependency of linear refractive index on the photon energy, $(E = h\upsilon)$, is given by Wemple and DiDomenico equation (see section 4.4.2)

4. Results and Discussion

4.1. Density and molar volume

The calculated density (ρ) and the molar volume (V_m) of the studied glasses were obtained from the expressions [23,24]:

$$\rho = \frac{x\,M_{V_2O_5}\,\rho_{V_2O_5} + (0.3-x)M_{Li_2O}\,\rho_{Li_2O} + 0.7M_{P_2O_5}\,\rho_{P_2O_5}}{x\,M_{V_2O_5} + (0.3-x)M_{Li_2O} + 0.7M_{P_2O_5}} \qquad (1)$$

$$V_m = \frac{M_{wt}}{\rho} \qquad (2)$$

where (M_{Li_2O}), $(M_{P_2O_5})$ and $(M_{V_2O_5})$ are the molecular weights of (Li_2O), (P_2O_5) and (V_2O_5). Moreover, (ρ_{Li_2O}), $(\rho_{P_2O_5})$ and $(\rho_{V_2O_5})$ are the densities of (Li_2O), (P_2O_5) and (V_2O_5) (2.01, 2.39, and 3.36 g/cm^3 respectively). On the other hand, (M_{wt}) is the total molecular weight of each sample. The calculated data for the molar volume and the density are tabulated in Table (2).

Table (2): shows the molecular weight (M), the density (ρ), the molar volume (V_m) and the number of molecules per unit volume (N) of the studied glasses

Glass Samples	Density (g/cm^3)	Molecular Weight (g/mole)	Molar Volume V_m (cm^3/mole)	$N(\times 10^{22})$ (cm^{-3})
S_0	2.373	108.298	45.637	1.319
S_1	2.375	108.602	45.727	1.316
S_2	2.377	108.906	45.816	1.314
S_3	2.382	109.818	46.103	1.306
S_4	2.391	111.339	46.565	1.293

The density, molecular weight and molar volume of the samples are observed to increase with increasing the dopant content of V_2O_5 and decreasing the Li_2O content. While the number of molecules per unit volume (N) decrease with increasing V_2O_5. Consequently, the density and the molar volume of the studied glass samples are strongly dependent on the vanadium pentoxide content. The glass network thus tends to break off the bridging oxygen bonds leading to subsequent formation of non-bridging bonds [25,26]. Hence, it can be inferred that the intercalation of V_2O_5 in $[Li_2O - P_2O_5]$ glass causes the structural change in the glass network.

4.2. Refractive Indices Determination

It is established fact that when light passes through glass, it is divided into processes transmission, absorption and reflection; the following formula must be verified:

$$T + R + A = 1 \qquad (3)$$

where (T) is the transmittance, (R) is the reflectance and (A) is the absorbance of the material.

Based upon measured data, the obtained results for reflectance and transmittance are displayed in Fig. (2). The experimental spectral reflectance of the prepared glasses with different concentrations of V_2O_5 is illustrated in Fig. (2.a). On the other hand, Fig. (2.b). shows the experimental spectral transmittance of the prepared samples with various concentrations of V_2O_5.

Alternatively, earlier studies [e.g.27] proposed as an approximation: the relation between the measured (R), (T) and interface (Fresnel) reflectance (R_{as}), as

$$R_{as} = \frac{[2+T^2-(1-R)^2]-\{[2+T^2-(1-R)^2]^2-4(2-R)R\}^{1/2}}{2(2-R)} \qquad (4)$$

This leads to deduces the imaginary part of the refractive index (k) from

Fig. (2): Measured (a) reflectance (R), (b) transmittance (T); of the different prepared glasses vs. wavelength

$$k = \frac{\lambda}{4\pi t} \ln\left[\frac{TR_{as}}{(R-R_{as})}\right] \quad (5)$$

and the absorption coefficient (α) can be written as

$$\alpha = \frac{4\pi k}{\lambda} \quad (6)$$

where (λ) is the wavelength of light used and (t) is the glass sample thickness.

Alternatively, the real part of the refractive index

$$n = \frac{(1+R_{as})}{(1-R_{as})} + \left[\frac{4R_{as}}{(1-R_{as})^2} - k^2\right]^{1/2} \quad (7)$$

In this work, several analytical expressions are utilized to retrieve the real and imaginary refractive indices; while taking into consideration incoherent multiple reflections inside the sample.

Equations (4, 5 and 7) are used to obtain the real (n) and imaginary (k) refractive index of the studied glasses, from the overall measured reflectance and transmittance of the glass samples. The refractive index dispersion obeys, to a great extent, Sellmeier's empirical dispersion equation:

$$n^2(\lambda) = 1 + \sum_i \frac{B_i \lambda^2}{\lambda^2 - C_i} \quad (8)$$

where (B and C) are experimentally determined Sellmeier coefficients.

Figure (3.a). shows the behavior of the real part of refractive index (n) of studied glass samples within the range 200-2500 nm. On the other hand, Figure 3.b. shows the behavior of the imaginary part of refractive index (k) of studied glass samples within the range 200-2500 nm.

It can be inferred that, the accommodation of V_2O_5 readily changes the refractive index (n) of the samples nonlinearly.

Fig (3): Measured (a) real refractive index (n), (b) imaginary refractive index (k); of the different prepared samples vs. wavelength (λ)

4.3. Determination of the Dielectric Constant

The complex dielectric function (ε), representing the underlying molecular mechanism, is an indication for the interaction of EM waves with matter [28]. The components of the complex dielectric constant (ε_1, ε_2) of a material, are expressed in terms of the optical constants (n) and (k); such that the real part

$$\varepsilon_1 = n^2 - k^2 \qquad (9)$$

and the imaginary part is

$$\varepsilon_2 = 2nk \qquad (10)$$

Figure 4.a. shows the real part of the dielectric constant, (ε_1), versus the photon energy (hν) for the studied samples. For all samples the dielectric constants shows an exponential increase with photon energy and randomly change with the increase of the ratio of V_2O_5. This means that the free carrier concentration of the different glass compositions change in the different manner with the change in V_2O_5 content. Sample (S_2) has the highest, (ε_1), while sample (S_1) has the lowest, (ε_1). On the other hand, Fig. (4.b). shows the imaginary part of the dielectric constant, (ε_2), versus the photon energy for the same glass compositions. Such determination of the imaginary part of dielectric constant could be employed in determination of the optical relaxation time of glasses.

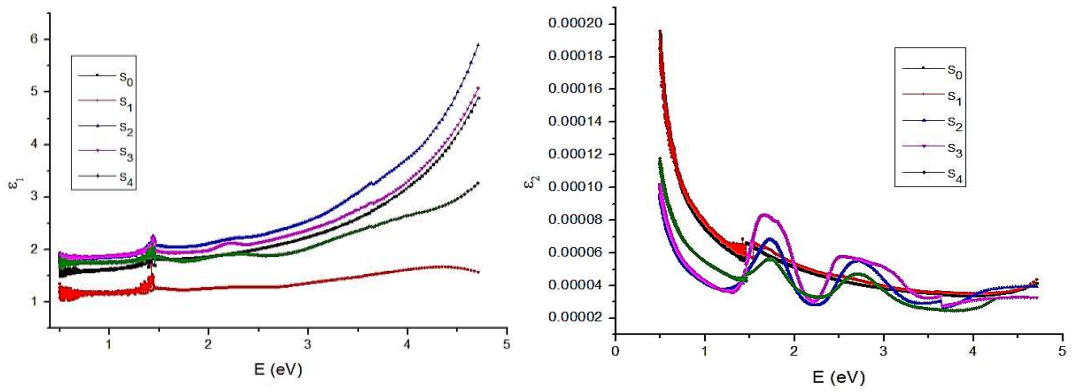

Fig. (4): Measured (a) real , (b) imaginary parts of dielectric constant vs. photon energy.

4.4. Equations for Linear Refractive index Dispersion

4.4.1. Abbe's Number

In glass manufacturing, for chromatic aberration correction, the material dispersion of any glass is described by the Abbe's number, (v_d) which is given by [21,29]:

$$v_d = \frac{n_d - 1}{n_F - n_C} \tag{11}$$

where $(n_F, n_C \text{ and } n_d)$ are the linear refractive indices at the standard wavelengths: (λ_F, λc and λ_d), Respectively F-line is the blue line (λ=479.98nm), the c-line is the red line (λ=643.8nm) from the cadmium spectrum and d-line is yellow line (λ_d =587.56nm) from the He spectrum. The refractive indices difference $(n_F - n_C)$ is called the mean dispersion. Moreover, materials which have low refractive indices usually have a high Abbe's number and therefore exhibit low dispersion. Traditionally, the reciprocal of Abbe's number (v_d) represents the dispersive power of a glass material.

4.4.2. The Wemple-DiDomenico dispersion relation

Wemple & DiDomenico (W-D) [30,31] laid a design for the (n) data in a single oscillator model, as a function of the incident photon energy (E) in the transparent region as

$$n^2 - 1 = \frac{E_0 E_d}{E_0^2 - E^2} \tag{12}$$

where (E_0) is the so called Sellmeier energy gap [21,32] and (E_d) is the dispersion energy. Conventionally, The single oscillator energy (E_0) is related to the average band gap and corresponds to the distance between the centers of gravity of the CB and VB. (E_d), it is the average strength of interband optical transitions represents average excitation energy for electronic transitions as well as the electronic oscillator strength related to dispersion.

The linear fitting of $(n^2 - 1)^{-1}$ versus (E^2) is suitable to find (E_0) and (E_d) from

$$\frac{1}{n^2-1} = \frac{E_0}{E_d} - \frac{E^2}{E_0 E_d} \quad (13)$$

Alternatively the refractive index at infinite wavelengths, considering only electronic transitions, can be written as

$$n_\infty = \sqrt{1 + \frac{E_d}{E_0}} \quad (14)$$

4.5. The Reflection loss (R %)

The energy loss of the incident light, from the glass surface, by reflection is defined as Reflection loss. In due course, it leads to important measurements concerning light transmission characteristics for various colors of glasses. Basically, the fraction reflected by a single surface can be calculated from Fresnel's formula (specifically in case of normal incidence of light on a glass surface). The reflection losses (R %) of each glass sample can be determined from [21,29] :

$$R\,\% = \left[\frac{(n_e - 1)}{(n_e + 1)}\right]^2 \times 100 \quad (15)$$

where (n_e) is the glass refractive index at $\lambda = 546.1$nm.

4.6. Molar Refractivity and Polarizability

The molar refractivity (R_M), basically deduced from the refractive index (n_e), molecular weight (M), and the density (ρ) of the studied glass [21,29], is given as:

$$R_M = \frac{(n_e^2 - 1)}{(n_e^2 + 2)} \left(\frac{M}{\rho}\right) \quad (16)$$

From equation (16) and using the Clausius-Mossotti equation [21,33,34], the polarizability (α_m) is calculated from:

$$R_M = \frac{4\pi N_A}{3} \alpha_m \quad (17)$$

where (N_A) is Avogadro's number

Table (3): The measured indices (n_F, n_D and n_C), Abbe's number (v_d), the mean dispersion, the dispersive power of a glass material, reflection loss (R%), the molar refractivity (R_M) and polarizability (α_m) of the glass samples. The measured optical parameters change randomly as the V_2O_5 content increases.

Glass Sample	n_F	n_D	n_C	n_e	v_d	v_e	Mean dispersion	dispersive power	R%	R_M	α_m
S_0	1.4316	1.3777	1.3635	1.3935	5.7867	5.546	0.068	0.1728	0.02703	10.9044	4.321
S_1	1.1324	1.127	1.1184	1.1327	9.4785	8.881	0.014	0.1055	0.00387	3.94187	1.562
S_2	1.5182	1.471	1.4433	1.4891	6.53	6.288	0.0749	0.1531	0.03861	13.2256	5.24
S_3	1.474	1.440	1.4052	1.4582	6.6598	6.3953	0.0688	0.1501	0.03474	12.5845	4.986
S_4	1.3728	1.374	1.3507	1.3853	17.4343	16.923	0.0221	0.0573	0.02609	10.9201	4.327

Table (4): The dispersive results deduced from the (n) data of the studied samples. Parameters (E_d), (E_0) and (n_∞) changed randomly with the increase of the concentration of V_2O_5.

Glass Sample	E_d (eV)	E_o (eV)	n_∞
S_0	6.013	2.688	1.7991
S_1	3.175	5.905	1.24
S_2	3.98	4.71	1.3583
S_3	4.321	5.068	1.3611
S_4	4.082	5.505	1.3196

4.7 Glass Fermi Energy

As the imaginary refractive index, (k), has a steep edge towards the IR side of the spectrum, and can be represented by Fermi–Dirac distribution function [35,36]:

$$k = \frac{1}{1+\exp\left(\frac{E_F - E}{K_B T}\right)} \tag{18}$$

where (E_F) is the Fermi energy

The variable photon energy ($E = hc/\lambda$), the thermal energy at the moment of measuring the sample (k_BT), Planck's constant (h), light velocity in vacuum (c), Boltzmann constant (k_B) and the absolute temperature at the moment of measuring the sample spectra (T). Eq. (18) can be rewritten as:

$$K_B T \ln\left(\frac{1}{k} - 1\right) = E_F - E \tag{19}$$

The linear fitting of this equation was implemented to determine the glass Fermi energy.

4.8. The Optical Absorption Results

4.8.1. Optical Band Energy (E_{Og})

The absorption coefficient, (α), of each glass sample (as a function of the photon energy (E)) can be computed from the relation [37]:

$$\alpha E = B(E - E_{Og})^{m} \qquad (20)$$

The numerical value, (B), is a constant that essentially depends on the assessment of electron transition probability; commonly known as Tauc's law [38]. The value (B) is in the order of $10^5 cm^{-1}$ eV^{-1}. The power, m, is a characterizing number for the transition mechanism; $m = 1/2$ for allowed direct transition, m= 3/2 for direct forbidden and m = 2 for allowed indirect transition, m=3 for indirect forbidden transitions. the optical band gap energy is (E_{Og}). Plotting the relation between $(\alpha E)^{1/2}$ and (E) gives the direct band gap energy, (E_{Og-d}), while a relation between $(\alpha E)^{1/2}$ and (E) gives the indirect band gap energy, (E_{Og-i}) [31].

4.8.2. Urbach Energy

The values of the absorption coefficient lying between 10^2 -10^4 cm^{-1}, are defined as Urbach's exponential tail region [39] and are given by:

$$\alpha = \alpha_0 \exp\left(\frac{E}{E_U}\right) \qquad (21)$$

where (α_0) is a constant, (E) is basically the photon energy and (E_U) being the Urbach energy. (E_U) is commonly interpreted as the tail width of localized states, within the band gap.

Equation (21) can be rewritten as:

$$\ln \alpha = \ln \alpha_0 + \frac{E}{E_U} \qquad (22)$$

Hence, the Urbach energy is usually obtained from plotting the relation between the energy of photon (E) and the absorption coefficient's natural logarithm.

4.8.3. The steepness parameter

The broadening of the optical absorption edge due to exciton-phonon or electron phonon interaction at room temperature, T=300 K, is characterized by the steepness parameter [36,40]:

$$S = \frac{K_B T}{E_U} \qquad (23)$$

where (K_B) is the Boltzmann constant

Table (5): The indirect allowed optical energy gap ($E_{in-\ direct}$), the empirical gap (E_{g-em}), the Urbach energy (E_U), the Fermi energy (E_F) and the steepness parameter (S) of the samples.

Glass Sample	$E_{in-\ direct}$ (eV)	E_f(eV)	E_u(eV)	E_{g-em}(eV)	S
S_0	6.275	2.154	2.275	3.671	11.373×10^{-1}
S_1	5.218	2.720	3.261	4.426	7.934×10^{-3}
S_2	2.706	2.383	3.238	3.440	7.991×10^{-3}
S_3	3.254	2.358	3.092	3.512	8.368×10^{-3}
S_4	4.351	2.352	4.050	3.692	6.388×10^{-3}

The indirect optical band gap values (as seen in Table 5) are observed to change nonlinearly upon increasing the V_2O_5. The nonlinear change in these values may be attributed to the effect of V_2O_5 concentration; which can alter and enhance the formation of NBOs in the glass network.

4.9 Predicted Nonlinear Optical Parameters

In order to evaluate the non-linear part of the refractive index, (n_2), the following empirical formula [29,31] is applied:

$$n_2(e^{-13}\,esu) = \frac{68\,(n_e - 1)(n_e^2 + 2)^2}{v_d\left[1.517 + \frac{(n_e - 1)(n_e^2 + 2)}{6\,n_e}\,v_d\right]^{1/2}} \qquad (24)$$

where (n_e) is the refractive index at (λ_e) = 546.1nm and (v_d) is the Abbe number for the studied samples. From Boiling's semi-empirical equation [41], the 3rd order susceptibility (χ^3) of the nonlinear part index of refraction, is written as

$$\chi^3(e^{-13}\,esu) = \frac{n_\infty\, n_2}{12\,\pi} \qquad (25)$$

Moreover, the non-linear refractive index coefficient (γ) is given by

$$\gamma(cm^2/W) = \frac{4\,\pi \times 10^7}{c\,n_e} n_2\,(esu) \qquad (26)$$

where (c) is the velocity of light.

Table (6): The predicted nonlinear optical parameters

Glass Samples	$n_2\ (e^{-13}esu)$	$\chi^3(e^{-13}esu)$	$\gamma(e^{-13}esu)$
S_0	46.984	2.241	14.128
S_1	7.581	0.249	2.804
S_2	54.601	1.966	15.365
S_3	48.718	1.758	14.000
S_4	11.097	0.388	3.356

The studied samples show random change in the values of the non-linear parameters. Then as the concentration of V_2O_5 increases, the values of the non-linear parameters change randomly. The calculated accuracy of the non-linear optical parameters is ±0.001.

5. Conclusions

Vanadium-Lithium-Phosphate [V_2O_5-Li_2O-P_2O_5] glass samples were prepared by the technique of melt-quenching. The following deductions are evoked from this study:

1. The amorphous nature of these glasses was verified through XRD examination at room temperature.
2. The density of samples increased from 2.373 − 2.391 g/cm^3 as the V_2O_5 content was increased.
3. Upon doping with various V_2O_5 concentrations, linear and non-linear optical parameters indicated an anomalous behavior of the samples. Thus dispersion parameters can be controlled by the doping concentration of V_2O_5.
4. The glass sample (S_1), doped with 0.2 % (V_2O_5), exhibits reduced values of (E_d) and (n_∞).
5. In addition, glass sample (S_1) shows lower values of: reflection loss, mean dispersion, dispersive power of a glass material, molar refractivity and polarizability.
6. For glass sample (S_2), similarly doped with 0.4 % (V_2O_5), lower values of (E_{og}), indicate that the covalent bonding nature decreases with increasing the concentration of V_2O_5.
7. Moreover, glass sample (S_1), doped with 0.2 % (V_2O_5), displays lower values for : non-linear optical parameters , the 3rd order susceptibility and the non-linear refractive index coefficient.

The above deduced inferences find contemporary applications based on the phenomena of non-linearity in modified glass matrices, namely; laser glass with low nonlinear refractive index as well as optical switching with high refractive index.

References

1. Jayasankar C K Babu P Troster Th and Holzapfel W B 2000 *J.Lumin*. **91** 33
2. Lakshmikantha R Rajaramakrishna R Anavekar R V and Ayachit N H 2012 *CAN. J. PHYS.* **90(3)** 235-239
3. Brow R K 2000 *J. Non-Cryst. Solids* **263-264** 1-28
4. Reis S T Faria D L A Martinelli J R Pontuschka W M Day D E Partiti C S M 2002 *J. Non-Cryst. Solids* **304** 188

5. Van Wazer J R *Interscience* 1958 *New York* 1
6. Moss R M *Ph.D. thesis Dept. Physics Kent Univ Canterbury England* 2009
7. Mirzayi M and Hekmatshoar H M *Ionics* 2009 **15** 121-127
8. Vedeanu N Cozar O Ardelean I and Ioncu V 2007 *J. Optoelectron. Adv. Mater* **9** 844-847.
9. Stoch P Stoch A Ciecinska M Krakowiak I 2016 *J. Non-Cryst. Solids* **450** 48–60
10. Brow R K Click C K and Alam T M 2000, *J. Non-Cryst. Solids* **274** 9
11. ElBatal H A Abdelghany A M ElBatal F H ElBadry K M and Moustaffa F M 2011, *Physica B*, **406** 3694-3703
12. [12]ElBatal F H Hamdy Y M and Marzouk S Y 2009 *J. Non-Cryst. Solids* **355** 2439-2447
13. Ardelean I Dorina Rusu Andronache C and Ciobotă V 2007 *J.matlet.* **61** 3301–3304
14. Ivascu C Timar Gabor A Cozar O Daraban L Ardelean I 2011 *j.molstruc*. **993** 249‑253
15. Mercier C Palavit G Montagne L Follet-Houttemane C 2002 *C. R. Chimie* **5** 693–703
16. Chahine C Et-Tabirou M Pascal J L 2004 Mater. **58** 2776–2780
17. Bih L Omari ME Reau J-M Haddad M Boudlich D Yacoubi A Nadiri A 2000 *Solid State Ion* **132** 71–85
18. Bacewicz R Wasiucionek M Twarog A Filipowicz J Jozwiak P Garbarczyk J 2005 *J. Mater Sc*i **40** 4267–4270
19. Reddy CN Asokan S Anavekar RV 2007 *Mater. Sci* **30** 65–68
20. Ardelean I Cozar O Vedeanu N Rusu D Andronache C 2007 *J.Mater Sci Mater Electron* **18** 963–966
21. El Sayed Said Yousef 2014 *Solid State Phenomena **207** 1-35*
22. Al- Ani S Hogarth C J 1987 *Matter Sci* Lett. **6** 519
23. Barczynski R J 2005 *Opt. Appl*. **35** 875–879
24. Lee S Maeda H Obata A Ueda K Narushima N Kasuga T J.2015 *Ceram. Soc*. Jpn. **123** 942–948
25. Vijaya Kumar B Sankarappa T Prashant Kumar M Kumar S 2009 *J. Non-Cryst. Solids* **355** 229-234
26. Al-Hajry A Tashtoush N El-Desoky M M 2005 *Physica B* **368** 51–57
27. Nichelatti EJ 2002 *Opt A Pure Appl Opt* **4** 400
28. Kremer F 2002 *J. Non-Cryst. Solids* **305** 1
29. Annapurna K, Buddhudu S 1991 *J Solid State Chem* **93** 454
30. Wemple SH DiDomenico M 1971 *Phys Rev B* **3** 1338
31. El-Zaiat SY 2014 *Opt Rev* 21-54
32. Hoon Kim S Yoko T Am J 1995 *Ceram* **78** 2486
33. Clausius R 1879 Die mechanischeU'grme theorie **2** 6220.
34. Mossotti OF 1850 *Mem dimathem efisica in Modena* **24** 11-49.
35. Jiles D 1994 *Chapman & Hall,London*

36. El-Naggar A M El-Zaiat S Y Youssif M I Alsaud F A 2013 *j.optmat* **35** 2685‑2690
37. Davis EA, Mott NF 1970 *Philos Mag* **22** 3-9
38. Tauc J Grigorovici R Vancu A 1966 *J Phys Stst Sol* **15** 627
39. Urbach F 1953 *Phys Rev* **92** 1324
40. Mahr M 1962 *Phys Rev* **125** 1510
41. Vogel EM Weber MJ Krol DM 1991 *Phys Chem Glasses*